J Physiol Sci (2012) 62:21–28
DOI 10.1007/s12576-011-0182-7

ORIGINAL PAPER

Variable open-end wave reflection in the pulmonary arteries of anesthetized sheep

Nathan Dwyer · Ah Chot Yong · David Kilpatrick

Received: 1 August 2011 / Accepted: 9 November 2011 / Published online: 20 November 2011

Abstract The aim of this study was to re-evaluate wave reflection in the healthy pulmonary arteries of sheep utilizing the time-domain-based method of wave intensity analysis. A thorough understanding of patterns of wave reflection during health and disease may provide future sensitive markers of early pulmonary vascular disease. Wave intensity was calculated from the simultaneous acquisition of proximal pulmonary arterial pressure and velocity in 12 anesthetized open-chest sheep. Normal pulmonary arterial wave speed was 2.1 ± 0.3 m s^{-1}. The incident forward compression wave generated by right ventricular systole was reflected in an open-end manner as a backward expansion wave from a site 3 cm downstream, corresponding to the main pulmonary bifurcation, and in a closed-end manner as a backward compression wave from a site 21 cm downstream, corresponding to the pulmonary microcirculation. The proximal open-end reflection site was not present throughout the entire cardiac cycle. Wave reflection was minimal with only 1% of the incident forward compression wave energy reflected as a backward expansion wave and 2% as a backward compression wave. The normal pulmonary artery in open-chest sheep is characterized by variable proximal open-end reflection from the main pulmonary bifurcation and fixed closed-end reflection from the microcirculation, generating backward-travelling waves of minimal intensity.

N. Dwyer (✉) · A. C. Yong · D. Kilpatrick
Discipline of Medicine, University of Tasmania Clinical School, 43 Collins Street, Hobart, TAS 7000, Australia
e-mail: ndwyer@utas.edu.au

N. Dwyer · D. Kilpatrick
Department of Cardiology, Royal Hobart Hospital, Tasmania, Australia

Keywords Hemodynamics · Lung · Pulmonary artery · Wave intensity analysis · Wave reflection · Wave speed

Introduction

As the pulmonary circulation is highly compliant with a substantial ability to recruit blood vessels, 50–60% of the pulmonary microcirculation is diseased before a pressure rise is manifest [1]. An elevated mean pulmonary artery pressure is therefore a late manifestation of pulmonary vascular disease, and new techniques are required to define the condition in its earlier and perhaps more treatable stages. Experiments have indicated that right ventricular output decreases because of an increased afterload if, at any given resistance, pulmonary arterial compliance decreases and/or wave reflection increases [2, 3]. Quantification of the forward- and backward-travelling (reflected) wavefronts that drive pulmonary arterial flow may therefore serve as useful physiological markers of the status of the pulmonary circulation. In particular, prominent and/or early arrival of reflected wavefronts may be an early marker of pulmonary vascular disease.

Wave intensity analysis (WIA) is a recently developed time-domain technique utilizing high fidelity pressure (P) and velocity (U) measurements to determine the intensity, direction, type and timing of waves that may co-exist in a vascular system [4]. We have utilized WIA to identify and quantify the waves driving normal pulmonary arterial flow, as this technique has significant advantages over the prevailing impedance (frequency-based) methods, which include the excellent resolution of simultaneously existing forward- and backward-travelling waves as well as the ability to accurately determine multiple reflection sites [5].

Wave travel and reflection has been well characterized in the aorta and coronary arteries utilizing WIA [6–11]. In comparison, pulmonary arterial WIA has only been studied to a limited degree in animals, and there have been no human investigations published to date. The utility of WIA in resolving backward-travelling waves and providing insights into pulmonary arterial function was well demonstrated by Smolich et al. [12] in the fetal circulation of lambs. These authors showed that the mid-systolic fall in fetal pulmonary trunk blood flow was due, in part, to cyclical pulmonary vasoconstriction leading to a large backward compression wave (BCW).

Hollander et al. [13–15] were the first to utilize WIA to investigate wave travel in the pulmonary arteries of dogs. This group identified an early systolic backward expansion wave originating from an open-end reflection source considered to arise from the large increase in pulmonary vascular cross-sectional area occurring over a short distance. In these pioneering papers, descriptions and characterization of other backward waves evident in the figures were not reported. In particular, an early systolic backward wave arriving before the incident wave peak was unexplained.

It is now recognized that even small relative delays in velocity and pressure signal transmission, and to a lesser extent errors in calculated wave speed, may substantially exaggerate backward-travelling wave intensity or even introduce artificial waves [16]. Time lags between pressure and velocity signals occur because of hardware-related processing times, which may be as great as 26 ms for transit time flow meters depending on the model and filter frequency used [17]. Relative delays also result from difficulties in achieving exact co-location of sensors; at wave speeds of 2.0 m s^{-1}, a 1 cm difference in sensor locations would lead to a 5 ms signal delay.

Though Hollander et al. [13] determined the electronic delay of their flowmeter to be 3.5 ± 0.5 ms, less than one sampling interval at 200 Hz, no adjustment for this delay was made. Furthermore, other contributions to signal delay such as those introduced by difficulties in co-locating the pressure and velocity sensors were not accounted for. Pressure–velocity loops that can be used to precisely define any delays [17] were not utilized, which may have contributed to errors in the calculation of wave speed via the technique employed. Therefore, we reinvestigated wave travel in the normal pulmonary vascular bed of a different animal species utilizing WIA to confirm, describe, and quantify the presence of all of the reflected waves, if any, once pressure–velocity signal delays had been accurately accounted for. An understanding of wave travel in the healthy pulmonary artery is essential for our understanding of wave reflection in the diseased pulmonary vasculature.

Materials and methods

Experimental animals

Twelve healthy adult Polworth–Comeback cross sheep (7 males; weight 41.1 ± 5.8 kg) were studied. The experimental protocol was approved by the Animal Ethics Committee of the University of Tasmania (Project Number A9700) and met the standards of the National Health and Medical Research Council of Australia (NHMRC) animal usage guidelines.

Animal preparation and instrumentation

The sheep were anesthetized with sodium pentobarbitone (30 mg kg^{-1} bolus; maintenance 3–8 mg kg^{-1} h^{-1}) and ventilated with oxygen-enriched air at a tidal volume of 15 ml kg^{-1} and rate of 16–20 breaths/min (Engstrom Erica; Engstrom Medical, Sweden). A left thoracotomy was performed, the pericardium opened; and an appropriately sized transit-time ultrasonic flow probe (Triton Technology, San Diego, CA, USA) was mounted around the proximal main pulmonary artery 2 cm distal to the pulmonary valve. This signal was filtered on-line at 100 Hz and converted to velocity using pulmonary arterial cross-sectional area. A 7F micromanometer-tipped catheter (Model SPC 771S; Millar Instruments, Houston, TX, USA) was inserted antegrade through the wall of the pulmonary artery and positioned as close as possible to the flow probe. Left and right ventricular pressures were measured using 7F fluid-filled pigtail catheters (Medtronic, Minneapolis, MN, USA) introduced via the carotid artery and external jugular vein, respectively. A single electrocardiographic (ECG) lead was also recorded via a bio-amplifier (ML132; ADInstruments, Bella Vista, Australia). At the end of the experiment, the sheep was euthanized with an overdose of sodium pentobarbitone.

Data acquisition

Measurements

Hemodynamic parameters were allowed to stabilize for approximately 30 min after completion of surgery. Hemodynamic recordings of 15 s duration were made with the ventilator paused at end-expiration. All analogue signals were passed through anti-aliasing, low-pass filters with a cut-off frequency of 100 Hz and were then sampled at a frequency of 1 kHz using a MacLab 8S analogue-to-digital data acquisition system (ADInstruments). The data were subsequently analyzed using customized scripts for Matlab R2008b (The Mathworks, Natick, MA, USA).

Post acquisition signal processing

The pressure and velocity signals were filtered using a second-order 31-point Savitzky–Golay filter, which reduces signal noise with minimal influence on peak magnitudes and widths [18]. For each animal, 12 individual cardiac cycles were analyzed, using the ECG R wave as a fiducial marker, and the wave intensity data subsequently pooled.

Signal delays were identified and corrected by utilizing pressure–velocity (*P–U*) loops and use of the fundamental relation $\rho c = \mathrm{d}P/\mathrm{d}U$ [17, 19, 20] (Figs. 1 and 2). Wave speed may be calculated with least-squares linear regression from the slope of the *P–U* relationship during early systole. This is a time when wave reflection is assumed to be absent [21, 22]. The time-lag was determined from the shift in *U* relative to *P* required to generate a linear relationship in early systole, which achieved the same wave speed as derived from an independent single-point technique [23] (see below). This single-point method is not affected by time-lag as it is calculated over the entire cardiac cycle and therefore served as a strong internal check. On average, velocity lagged pressure by 18 ± 3 ms.

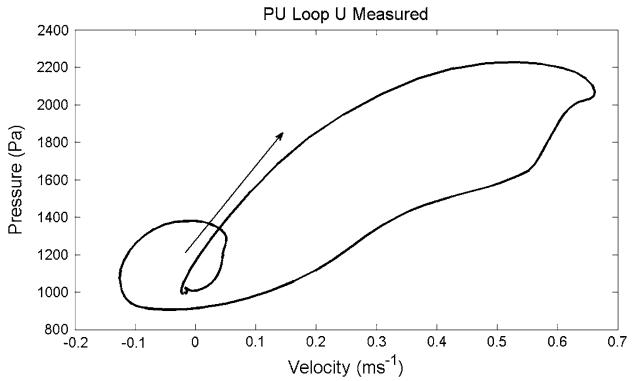

Fig. 1 A pressure–velocity (*PU*) loop for a single resting cardiac cycle without adjustments of the velocity signal delay. Velocity is lagging pressure by 20 ms, and in early systole (*arrow*), the loop is concave to the pressure axis. It is possible to see that wave speed calculated from $\mathrm{d}P/\mathrm{d}U \times 1/\rho$ in early systole would lead to an artificially high value and subsequently further errors in wave separation

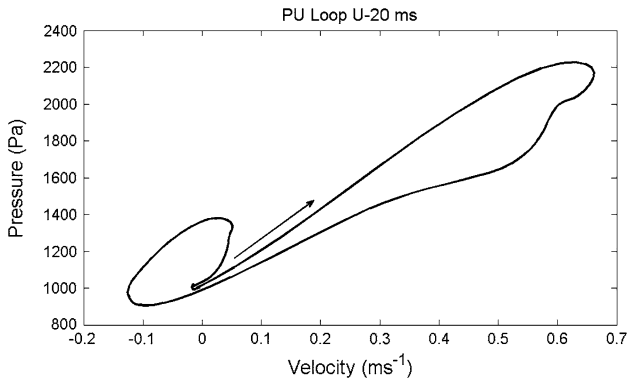

Fig. 2 A pressure–velocity (*PU*) loop for a single resting cardiac cycle with the velocity signal delay reduced by 20 ms. In early systole (*arrow*), there is now a linear relationship between *P* and *U* as predicted by the water hammer equation, and wave speed can now be accurately determined and compares favourably to the independent single-point technique

Wave types

The technique of WIA utilizes simultaneously acquired pulmonary pressure and velocity recordings to identify forward-travelling waves (originating upstream from the right ventricle) and backward-travelling waves (reflected waves originating downstream in the pulmonary circulation). These waves serve to either accelerate or decelerate the flow of blood in the forward direction depending on the nature and direction of travel of the wave (Table 1). A compression wave is identified by an increase in pressure across the wavefront and will accelerate blood velocity when originating from the right ventricle, but will decelerate blood velocity when originating distally. An expansion wave is identified by a drop in pressure across the wavefront and has a "suction" effect such that these waves will accelerate blood velocity when originating distally and will decelerate blood velocity when originating from the right ventricle.

Calculation of wave speed

Wave speed was determined locally at the point of pressure and velocity measurements utilizing a single-point technique across complete cardiac cycles [23]:

$$c = \frac{1}{\rho}\sqrt{\frac{\sum \mathrm{d}P^2}{\sum \mathrm{d}U^2}}$$

Table 1 Wave type, origin and nature

Wave type	Pressure	Velocity	Wave origin	Wave nature
Compression	↑	↑	Right ventricle (forward)	Accelerating
Compression	↑	↓	Pulmonary artery (backward)	Decelerating
Expansion	↓	↓	Right ventricle (forward)	Decelerating
Expansion	↓	↑	Pulmonary artery (backward)	Accelerating

Calculation of wave intensity

Wave intensity was separated into forward- (dI_+) and backward-travelling (dI_-) intensity components utilizing the following formulae [4]:

$$dI_+ = (dP/dt + \rho c dU/dt)^2/(4\rho c)$$

$$dI_- = -(dP/dt - \rho c dU/dt)^2/(4\rho c)$$

where dP and dU are the incremental changes in pulmonary artery pressure and velocity respectively over a sampling interval, ρ is the density of blood (assumed to be 1,030 kg m^{-3}) and c is the wave speed. A compression wave is identified when $dP > 0$ and an expansion wave when $dP < 0$.

By utilizing the first time derivatives of pressure and velocity, our results are independent of the sampling frequency used and allow comparisons between studies [24].

Peak wave intensity (W m^{-2} s^{-2}) and cumulative wave intensity (W m^{-2} s^{-1}), calculated by integrating the respective intensity over its duration, were determined for each wave. The proportion of cumulative wave intensity was calculated by expressing the cumulative wave intensity of an individual wave as a percentage of total cumulative wave intensity in the cardiac cycle.

Wave reflection

The distance to the site of wave reflection was calculated as the product of wave speed and one-half the time interval between the peaks of an incident forward-travelling wave and a backward-travelling (reflected) wave [16]. The magnitude of wave reflection was determined from the reflection coefficient, defined as the ratio of an individual backward wave's cumulative intensity to its incident forward wave's cumulative intensity. A negative reflection coefficient indicates open-end reflection resulting in a change of wave type from compression to expansion or vice versa. With closed-end reflection, there is no change of wave type. Assuming constant distensibility, the ideal ratio of daughter-to-parent areas (A_R) such that no reflection occurs is between 1.1 and 1.2 [22, 25]. When A_R falls below 1.1, the magnitude of positive closed-end reflection increases. When A_R increases above 1.2, the magnitude of negative open-end reflection increases [26].

Statistical analysis

All analyses were performed using Matlab R2008b (The Mathworks). Continuous variables are reported as mean ± 1SD. Independent one-sample t tests were used (with a null hypothesis mean = 0) and $p < 0.05$ was considered significant.

Results

Five predominant waves were identified over a cardiac cycle. All the forward- and backward-travelling waves dissipate during diastole (Fig. 3). The resting hemodynamic parameters are shown in Table 2. The normal pulmonary arterial wave speed was 2.1 ± 0.3 m s^{-1}. Whilst the peak intensity, timing, and cumulative wave intensity values of the individual waves varied between animals, when expressed as a proportion of total cumulative wave intensity less variation was manifest (Table 3).

Four distinct phases of right ventricular ejection were distinguished (Fig. 3):

1. An early forward compression wave (eFCW) accounting for acceleration of blood in the pulmonary artery.
2. An intervening period of near zero intensity during mid-ejection, where there is no change in blood acceleration.
3. A forward expansion wave (FEW), which may develop slowly (resulting in a broad wave) and which decelerates the blood volume ejected into the pulmonary artery, occurred 208 ± 23 ms after the eFCW.

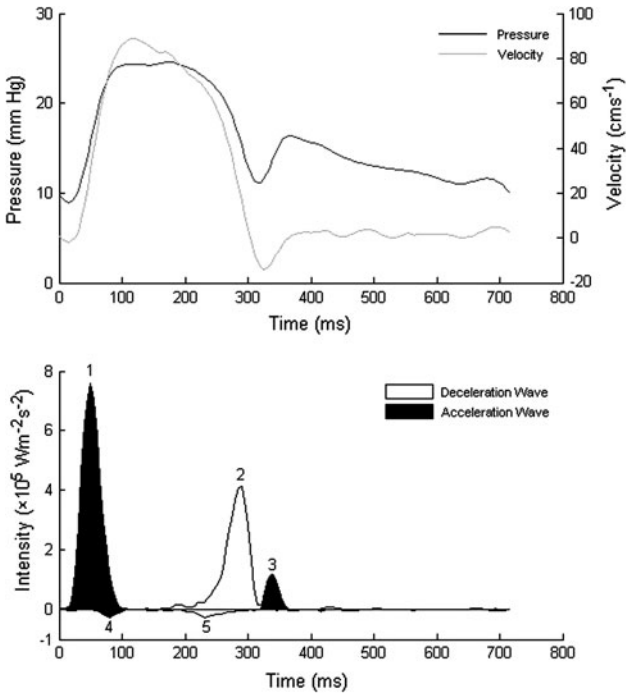

Fig. 3 Wave intensity in the proximal pulmonary artery with corresponding pressure and velocity traces over a single cardiac cycle. Negative wave intensity indicates backward-travelling waves. *1* An early forward compression wave; *2* a forward expansion wave; *3* a late forward compression wave; *4* a backward expansion wave; *5* a backward compression wave. *Black* waves that accelerate forward flow (forward compression and backward expansion waves); *white* those waves that decelerate forward flow (forward expansion and backward compression waves)

Table 2 Baseline hemodynamic parameters

Parameters	Values
Heart rate (min^{-1})	92 ± 7
Cardiac output (L min^{-1})	3.6 ± 0.9
Mean PA pressure (mmHg)	15.6 ± 3.0
RVSP (mmHg)	25.7 ± 16.8
RVEDP (mmHg)	1.6 ± 4.3
LVSP (mmHg)	120.0 ± 14.0
LVEDP (mmHg)	5.6 ± 2.5
PVR (Wood units)	2.8 ± 1.6
PaO_2 (mmHg)	100 ± 2

Values are mean ± SD; $n = 12$

LVEDP left ventricular end diastolic pressure, *LVSP* left ventricular systolic pressure, *PA* pulmonary artery, PaO_2 systemic arterial partial pressure of oxygen, *PVR* pulmonary vascular resistance, *RVSP* right ventricle systolic pressure, *RVEDP* right ventricular end diastolic pressure

Table 3 Pulmonary arterial wave intensity parameters

Parameters	Values	*P*
Peak wave intensity ($\times 10^4$ W m^{-2} s^{-2})		
Early forward compression	78.7 ± 43.3	<0.0001
Forward expansion	23.1 ± 12.5	<0.0001
Late Forward compression	3.3 ± 2.9	<0.0001
Backward expansion	1.3 ± 1.5	<0.0001
Backward compression	1.4 ± 1.1	<0.0001
Cumulative wave intensity ($\times 10^2$ W m^{-2} s^{-1})		
Early forward compression	238.0 ± 108.0	<0.0001
Forward expansion	117.2 ± 56.1	<0.0001
Late forward compression	9.2 ± 6.5	<0.0001
Backward expansion	2.7 ± 3.4	<0.0001
Backward compression	4.6 ± 3.4	<0.0001
Proportion of cumulative wave intensity (%)		
Early forward compression	62.7 ± 10.0	<0.0001
Forward expansion	31.6 ± 9.4	<0.0001
Late forward compression	3.2 ± 2.7	<0.0001
Backward expansion	1.0 ± 1.2	0.0001
Backward compression	1.5 ± 1.3	<0.0001
Wave speed (m s^{-1})	2.1 ± 0.3	<0.0001
Peak blood velocity (m s^{-1})	0.88 ± 0.01	<0.0001
Distance to reflection site (cm)		
Backward expansion	2.9 ± 0.8	<0.0001
Backward compression	21.2 ± 4.4	<0.0001
Reflection coefficient		
BEW/eFCW	−0.01 ± 0.01	0.45
BCW/eFCW	0.02 ± 0.01	0.0005

Values are mean ± SD; $n = 12$

BCW backward compression wave, *BEW* backward expansion wave, *eFCW* early forward compression wave

4. A late forward compression wave appeared 287 ± 31 ms after the eFCW and 76 ± 23 ms after the FEW.

Two backward-travelling waves were identified (Fig. 3):

1. An expansion wave appeared 28 ± 8 ms after the eFCW. The cumulative wave intensity was $2.7 \pm 3.4 \times 10^4$ W m^{-2} s^{-2} ($p = 0.0001$). The early forward compression wave (dP_+) was reflected as an expansion wave (dP_-) indicating open-end wave reflection. The reflection site was 2.9 ± 0.8 cm downstream with a reflection coefficient of −0.01 ± 0.01 (Table 3).
2. A compression wave appeared 207 ± 43 ms after the eFCW. The cumulative wave intensity was $4.6 \pm 3.4 \times 10^4$ W m^{-2} s^{-2} ($p < 0.0001$). The early forward compression wave (dP_+) was also reflected as a compression wave (dP_+) indicating closed-end reflection. The reflection site was 21.2 ± 4.4 cm downstream with a reflection coefficient of 0.02 ± 0.01 (Table 3).

Discussion

Previously reported peak intensity of the early forward compression wave (eFCW) was 60.0×10^4 and 44.0×10^4 W m^{-2} s^{-2} for the FEW in the pulmonary artery of dogs [13], which compares favorably with the present results. It is possible to normalize the intensity to the sampling interval (convert W m^{-2} to W m^{-2} s^{-2}) by multiplying the intensity value by the sampling frequency in hertz squared. A late forward compression wave (FCW) was also identified, which is mostly likely due to deceleration of the ejected volume of blood that momentarily reverses and is reflected from the closed pulmonary valve in the forward direction.

Like Hollander et al. [14], we identified a backward expansion wave (BEW) that arrives in the proximal pulmonary artery in early systole and arises from a similar site 2.9 ± 0.8 cm downstream, where it appears that the proximal pulmonary bifurcation behaves as an open-end reflector. This wave would have a physiological benefit by aiding the ejection of blood from the right ventricle at a lower energy cost, a clear advantage during high pulmonary flow situations such as exercise. The presence of a BEW implies that the cross-sectional area of the left and right pulmonary arteries is greater than the main pulmonary trunk. This is contrary to previous observations where their combined area was 10% smaller [27]. However, these calculations were made on pulmonary arterial casts in eight dogs and may not represent the in vivo geometry. The

notion that the pulmonary artery behaves as an open-end reflector is supported, however, by studies in isolated perfused lungs that demonstrate an A_R of 1.2–1.3 [28, 29], a ratio that leads to open-end reflection [25].

Only 1% of the incident eFCW energy was reflected as a BEW, which is significantly less than ~10% reported by Hollander et al. [14]. Interspecies variation may be an explanation for the difference, as it has been recognized that wave reflection in dogs is less than in humans [22], and therefore it is possible that there is greater spatial dispersion and less reflection in sheep. However, our higher sampling frequency and accurate account of pressure–velocity signal delay utilizing pressure–velocity loops likely explains the differences in observed backward-travelling wave energy. Indeed, if WIA is performed on the current data without accounting for signal delays, a larger BEW/eFCW reflection coefficient of −0.24 is obtained, indicating the artificial exaggeration of the BEW energy. Our data show that even a 5 ms velocity delay can lead to a 20% increase of the BEW intensity and a 30% increase in the reflection coefficient of the BEW/eFCW [30].

In addition, we have described a BCW arising 21.2 ± 4.4 cm downstream, corresponding to a closed-end reflection site, arriving in the proximal pulmonary artery during late systole. The BCW was frequently broad suggesting a more widespread and spatially diverse reflection site, which is in keeping with reflection from the terminal arterioles. Indeed, the existence of a distal reflection site from the peripheral microvasculature is supported by measurements that demonstrate a total arterial length of approximately 20 cm in the pulmonary circulation [31, 32].

The reflective coefficients of both backward-travelling waves were small. This may suggest that there are significant energy losses as a result of damping during wave travel, but it is more likely that, in the highly compliant, low resistance pulmonary circulation, wave reflection is minimized. Others have also shown that the right ventricle is well matched to its afterload [33]. Our data indicate only 1% of the incident eFCW was reflected as a BEW and a further 2% as a BCW. Whilst these backward-travelling waves carry little energy, they may still bear physiological significance, with their timing and intensity providing information about two different reflection sites and the status of the pulmonary circulation. For example, a high intensity BCW arising from the microcirculation may arrive early in systole, opposing flow out of the right ventricle in pulmonary vascular disease.

We have added to the observations of Hollander et al. [13, 14] by describing all the waves present, and propose that the proximal open-end reflector is not fixed throughout the entire cardiac cycle. If we assume that the open-end reflector is fixed in time, the eFCW would be reflected as a BEW, the FEW would be reflected as a BCW, and the late FCW would be reflected as a late BEW. However, our present data indicate that the BCW did not invariably follow the FEW (it sometimes preceded it), and we never observed a late BEW following the late FCW. Furthermore, the estimated distances to the proximal reflection site for the incident forward waves were different. If the eFCW is reflected as a BEW, the reflector site is 2.9 ± 0.8 cm downstream. If the FEW is reflected as a BCW, the reflector site is estimated to be 6.5 ± 3.9 cm downstream. The estimated distances should be very similar if reflected from the same site. Additionally, the reflection coefficients were different for the two incident waves. It was −0.01 ± 0.01 for the BEW/eFCW compared to −0.04 ± 0.03 for the BCW/FEW. The reflection coefficients should be similar if reflected from the same site.

These observations provide strong evidence that the open-end reflection is not fixed throughout the entire cardiac cycle. Open-end reflection may only be present during early systole when A_R is greater than 1.2, and then, as blood is emptied into the reservoir-like proximal pulmonary artery, A_R may fall to the theoretical value of 1.1–1.2 where no wave reflection occurs [25]. Indeed, it is easy to understand that conformational changes of the pulmonary vasculature occur throughout the cardiac cycle when the dynamic activities of the heart and blood vessels are observed in the open-chest sheep.

Furthermore, with accurate consideration of time delays in the current work, the problem of the presence of a physiologically meaningless early BCW arriving in the proximal pulmonary artery prior to the peak of the incident eFCW disappears (Fig. 4). It is possible that this otherwise

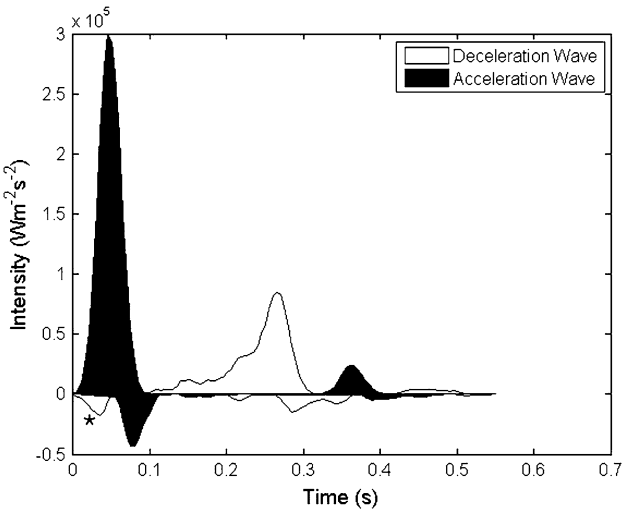

Fig. 4 Pulmonary arterial wave intensity analysis over a single cardiac cycle performed without adjustment of the velocity signal timing, demonstrating an unexplained early backward compression wave (*asterisk*). This physiologically meaningless wave disappears when pressure–velocity time delays have been accurately accounted for

unexplained early BCW could arise from retrograde transmission of left atrial pressure fluctuations. However, clamping two of the pulmonary veins did not attenuate this wave's intensity, and rapid right ventricular pacing did not alter the timing or appearance of this wave [30], suggesting that the early BCW does not arise from left atrial contraction. This wave was also unlikely to be an artifact related to a possible constricting effect of the cuff-like flow probe on the pulmonary artery, as this wave was detectable even when pressure was measured distal to the flow probe [30]. These observations make it likely that the early BCW wave seen in Hollander et al.'s [13, 14] and our unadjusted results is indeed an artifact related to delays between the pressure–velocity signals.

Limitations

Wave reflection may be different in anesthetized animals. However, patterns of impedance in conscious, unanesthetized dogs was similar to those in the anesthetized open-chest preparation [34], suggesting our qualitative interpretation of wave reflection in sheep would not be altered. However, the use of anesthetic agents that have negative inotropic effects and induce systemic vasodilatation may lead to quantitative changes. It is possible that wave speed and wave intensity are lower than in ambulatory animals. Furthermore, dissection of the adventitia in the proximal pulmonary artery may affect autonomic control of pulmonary vasculature tone and consequently wave speed in these open-chest animals.

Using a cuff-type flow probe may lead to errors in velocity determination if the velocity profile is not uniform across the vessel cross-sectional area. However, it seems from experimental data in humans and dogs that the pulmonary arterial velocity profile is symmetrical [35, 36]. The cuff-type flow probe may have constricted or minimized normal pulsatile distension, thus overestimating true pulmonary blood velocity, arterial pressure, and wave speed, and therefore overestimating cumulative wave energies. The assumption was made that the pulmonary artery was circular and that the cross-sectional area of the vessel was constant throughout the cardiac cycle, which leads to minor but constant errors in blood velocity calculations.

In addition, it is not certain that wave speed is constant throughout the cardiac cycle and across the pulmonary vasculature. This may lead to errors in determining the distances to reflection sites. However, our proposed reflection locations are anatomically plausible. The single-point technique for determining wave speed [23] has previously been criticized as being inaccurate in coronary arteries [37]. These issues do not appear relevant in the pulmonary artery, as similar wave speeds were also determined independently from pressure–velocity loops, therefore serving as an internal check.

The energy of wave travel is only a small part of the external work of the heart, which in turn is a fraction of the total energy expended by the heart. Therefore, whilst WIA gives an idea of the working state of the heart as well as downstream vascular reflective conditions, conclusions cannot be drawn about the optimal working state of the heart, only optimal patterns of wave travel that minimize opposition to right ventricular ejection.

Conclusions

The normal pulmonary arterial wave speed in sheep is 2.1 ± 0.3 m s^{-1}. The healthy pulmonary vasculature is characterized by minimal wave reflection with only $\sim$3% of the incident early forward compression wave energy reflected towards the right ventricle, attesting to the notion that the right ventricle and pulmonary circulation are well matched to minimize wave reflection. Two sites of wave reflection were consistently identified. The main pulmonary bifurcation behaves as an open-end reflector during early systole, leading to the generation of a backward expansion wave that would serve to enhance right ventricular emptying. The open-end reflector is not fixed throughout the entire cardiac cycle. The distal pulmonary microcirculation behaves as a closed-end reflector, leading to the generation of a BCW, serving to oppose flow out of the right ventricle. Although the intensities of these reflected waves are small, they may serve as important physiological markers of early pulmonary vascular disease, which will be explored in future experiments and ultimately in human subjects.

Acknowledgments Thanks to Prof. John Tyberg (University of Calgary, Canada) and Dr. Jiun-Jr Wang (Fu Jen Catholic University, Taiwan) for providing useful insights into the utility of wave intensity analysis. This work was supported by the National Health and Medical Research Council of Australia (K0016534 to N.D.).

Conflict of interest The authors declare that they have no conflict of interest.

References

1. Dalen JE, Haynes FW, Hoppin FG Jr, Evans GL, Bhardwaj P, Dexter L (1967) Cardiovascular responses to experimental pulmonary embolism. Am J Cardiol 20:3–9
2. Elzinga G, Piene H, de Jong JP (1980) Left and right ventricular pump function and consequences of having two pumps in one heart. A study on the isolated cat heart. Circ Res 46:564–574
3. Furuno Y, Nagamoto Y, Fujita M, Kaku T, Sakurai S, Kuroiwa A (1991) Reflection as a cause of mid-systolic deceleration of

pulmonary flow wave in dogs with acute pulmonary hypertension: comparison of pulmonary artery constriction with pulmonary embolisation. Cardiovasc Res 25:118–124
4. Parker KH, Jones CJ (1990) Forward and backward running waves in the arteries: analysis using the method of characteristics. J Biomech Eng 112:322–326
5. Wang J Jr, Shrive NG, Parker KH, Hughes AD, Tyberg JV (2011) Wave propagation and reflection in the canine aorta: analysis using a reservoir-wave approach. Can J Cardiol 27:e1–e10
6. Khir AW, Zambanini A, Parker KH (2004) Local and regional wave speed in the aorta: effects of arterial occlusion. Med Eng Phys 26:23–29
7. Jones CJH, Sugawara M, Kondoh Y, Uchida K, Parker KH (2002) Compression and expansion wavefront travel in canine ascending aortic flow: wave intensity analysis. Heart Vessels 16:91–98
8. Khir AW, Henein MY, Koh T, Das SK, Parker KH, Gibson DG (2001) Arterial waves in humans during peripheral vascular surgery. Clin Sci 101:749–757
9. Koh TW, Pepper JR, Desouza AC, Parker KH (1998) Analysis of wave reflections in the arterial system using wave intensity: a novel method for predicting the timing and amplitude of reflected waves. Heart Vessels 13:103–113
10. MacRae JM, Sun YH, Isaac DL, Dobson GM, Cheng CP, Little WC, Parker KH, Tyberg JV (1997) Wave-intensity analysis: a new approach to left ventricular filling dynamics. Heart Vessels 12:53–59
11. Davies JE, Whinnett ZI, Francis DP, Manisty CH, Aguado-Sierra J, Willson K, Foale RA, Malik IS, Hughes AD, Parker KH, Mayet J (2006) Evidence of a dominant backward-propagating "suction" wave responsible for diastolic coronary filling in humans, attenuated in left ventricular hypertrophy. Circulation 113:1768–1778
12. Smolich JJ, Mynard JP, Penny DJ (2008) Simultaneous pulmonary trunk and pulmonary arterial wave intensity analysis in fetal lambs: evidence for cyclical, midsystolic pulmonary vasoconstriction. Am J Physiol Regul Integr Comp Physiol 294:R1554–R1562
13. Hollander EH (1998) Wave-intensity analysis of pulmonary arterial blood flow in anesthetized dogs. PhD thesis, University of Calgary
14. Hollander EH, Wang JJ, Dobson GM, Parker KH, Tyberg JV (2001) Negative wave reflections in pulmonary arteries. Am J Physiol Heart Circ Physiol 281:H895–H902
15. Hollander EH, Dobson GM, Wang JJ, Parker KH, Tyberg JV (2004) Direct and series transmission of left atrial pressure perturbations to the pulmonary artery: a study using wave-intensity analysis. Am J Physiol Heart Circ Physiol 286:H267–H275
16. Khir AW, Parker KH (2002) Measurements of wave speed and reflected waves in elastic tubes and bifurcations. J Biomech 35:775–783
17. Swalen MJP, Khir AW (2009) Resolving the time lag between pressure and flow for the determination of local wave speed in elastic tubes and arteries. J Biomech 42:1574–1577
18. Savitzky A, Golay MJE (1964) Smoothing and differentiation of data by simplified least squares procedures. Anal Chem 36:1627–1639
19. Khir AW, Swalen MJP, Feng J, Parker KH (2007) Simultaneous determination of wave speed and arrival time of reflected waves using the pressure–velocity loop. Med Biol Eng Comput 45:1201–1210
20. Khir AW, O' Brien A, Gibbs JS, Parker KH (2001) Determination of wave speed and wave separation in the arteries. J Biomech 34:1145–1155
21. Dujardin JP, Stone DN, Forcino CD, Paul LT, Pieper HP (1982) Effects of blood volume changes on characteristic impedance of the pulmonary artery. Am J Physiol 242:H197–H202
22. Nichols WW, O' Rourke MF, McDonald DA (2005) Mcdonald's blood flow in arteries: theoretic, experimental, and clinical principles. Hodder Arnold, London
23. Davies JE, Whinnett ZI, Francis DP, Willson K, Foale RA, Malik IS, Hughes AD, Parker KH, Mayet J (2006) Use of simultaneous pressure and velocity measurements to estimate arterial wave speed at a single site in humans. Am J Physiol Heart Circ Physiol 290:H878–H885
24. Ramsey MW, Sugawara M (1997) Arterial wave intensity and ventriculoarterial interaction. Heart Vessels 12:128–134
25. Wang JJ (1997) Wave propagation in a model of the human arterial system. PhD thesis, University of London
26. Parker K (2009) An introduction to wave intensity analysis. Med Biol Eng Comput 47:175–188
27. Fry DL, Patel DJ, De Freitas FM (1962) Relation of geometry to certain aspects of hydrodynamics in larger pulmonary arteries. J Appl Physiol 17:492–496
28. Caro CG, Saffman PG (1965) Extensibility of blood vessels in isolated rabbit lungs. J Physiol 178:193–210
29. Collins R, Maccario JA (1979) Blood flow in the lung. J Biomech 12:373–395
30. Dwyer N (2010) Pulmonary arterial wave intensity analysis in health and disease. PhD thesis, University of Tasmania, Hobart
31. Singhal S, Henderson R, Horsfield K, Harding K, Cumming G (1973) Morphometry of the human pulmonary arterial tree. Circ Res 33:190–197
32. Horsfield K (1978) Morphometry of the small pulmonary arteries in man. Circ Res 42:593–597
33. Piene H, Sund T (1982) Does normal pulmonary impedance constitute the optimum load for the right ventricle? Am J Physiol Heart Circ Physiol 242:H154–H160
34. Milnor WR, Bergel DH, Bargainer JD (1966) Hydraulic power associated with pulmonary blood flow and its relation to heart rate. Circ Res 19:467–480
35. Reuben SR, Swadling JP, Lee GDJ (1970) Velocity profiles in the main pulmonary artery of dogs and man, measured with a thin-film resistance anemometer. Circ Res 27:995–1001
36. Caro CG (1978) The mechanics of the circulation. Oxford University Press, Oxford
37. Kolyva C, Spaan JAE, Piek JJ, Siebes M (2008) Windkesselness of coronary arteries hampers assessment of human coronary wave speed by single-point technique. Am J Physiol Heart Circ Physiol 295:H482–H490